

Accurate P-wave reflection and transmission coefficients for non-welded interface incorporating elasto-plastic deformation

Zihang Fan^{1,2,3}, Zhaoyun Zong^{*1,2,3} and Fubin Chen^{1,2,3}

⁽¹⁾ School of Geosciences, China University of Petroleum (East China), Qingdao, China, 266580.

⁽²⁾ Pilot National Laboratory for Marine Science and Technology (Qingdao), Qingdao, China, 266580.

⁽³⁾ Shandong Provincial Key Laboratory of Deep Oil and Gas, Qingdao, China, 266580.

Article history: received October 9, 2022; accepted September 6, 2023

ABSTRACT

P-wave reflection and transmission coefficients for non-welded interface play crucial roles in broad practical engineering productions, involving fracture properties prediction and seismic inversion. However, the existing reflection coefficient equations for non-welded interface in elasto-plastic media are seldom studied, although the elasto-plastic deformation is frequently encountered in the Earth's subsurface due to artificial and tectonic activities. In this study, we proposed the accurate reflection and transmission coefficients equation for a non-welded interface embedded in an elasto-plastic deformed medium based on the elasto-plastic acoustoelastic and linear-slip theory. In detail, this paper uses elasto-plastic acoustoelastic theory to derive the reflection and transmission coefficients equation. The reflection and transmission coefficients matrix are solved using the linear-slip theory as the boundary condition. Moreover, we use the hardening parameter and plastic deformation to represent the plastic properties of the rock, which is a function of stress and plastic deformation. Through Numerical analysis, the deformation caused by static stress has significantly changed the amplitude and the slope of the reflection and transmission coefficients amplitude. As the stress increases, the rock's velocity becomes higher, and all reflection and transmission coefficients (i.e., R_{PP} , R_{PS} , T_{PP} , T_{PS}) abruptly change at the critical angle. Furthermore, with the increase in plastic deformation, the critical angle of the incident P-wave and the hardening parameter becomes larger than the unstressed state. The non-welded interface exhibits a low-pass frequency filter for reflected SV-waves and a high-pass frequency filter for reflected P-waves and transmitted P and SV waves. In addition, we can observe that static vertical stress can weaken the anomalous reflections caused by non-welded formations, but the effect is insignificant. On the other hand, the effect of fracture normal compliance to reflection and transmission is detailly investigated. When $\Delta_N < 2.5 \times 10^{-10} (MPa^{-1})$, The non-welded interface is close to the welded interface, while $\Delta_N > 2.5 \times 10^{-5} (MPa^{-1})$, the non-welded interface is close to the solid-air interface.

Keywords: Non-welded interface; Liner-slip theory; Elasto-plastic deformation; Third-order elastic modulus; Acoustoelastic theory

1. INTRODUCTION

The fractures buried deep in the subsurface Earth are subject to the overburden pressure caused by the gravity of the overlying strata. This overburden vertical pressure usually affects the fracture's effect on the wave propagation and elasticity of the medium [Mulargia, 1979; Chen et al., 2021; Traylor, 2021], which can be reasonably described by the acoustoelasticity theory. The acoustoelasticity theory, also termed third-order non-linear elasticity theory, assumes the strain energy includes cubic term and quadric term in the classic elasticity theory [Hughes and Kelly, 1953; Norris 1998]. Acoustoelasticity was first used for stress detection and third-order elastic modulus prediction [Johnson, 1996]. Recently, acoustoelasticity was also used to study stress-related reflection and transmission responses [Liu, 2007, 2012; Chen, 2021a; Yang, 2022]. However, actual subsurface strata under the large loading possess elasto-plastic characteristics, which highly affect rock wave velocity and elasticity. In the meantime, the reflection and transmission coefficients are also greatly affected by the elasto-plastic. Therefore, considerable work has been carried out on wave reflection and transmission parameterization for the interfaces between elasto-plastic deformation media [David, 2012; Green and Naghdi, 1966a, 1966b]. Sinha [2001] considered the elasto-plastic deformation assumption to obtain a more accurate rock response. However, few people consider, when the interface is non-welded.

The discontinuous non-welded interface induced by fractures, cracks, and joints exists widely in the Earth's interior. The linear-slip theory can describe the discontinuity of non-welded interface with fracture compliances, which was first proposed by Schoenberg [1980]. Michael [1995] presented a simple method to represent the effect of natural fracture on seismic propagation and write the compliance tensor of the fractured rock as the sum of unfractured background rock's compliance tensor and parallel fractures or aligned fracture's compliance tensor. Johnson [1996] connected the wave's elastic nonlinearity and stress-induced effect. Chaisri [2000] derived the accurate equations for P-SV particle displacement reflection and transmission coefficients for plane waves incident upon the non-welded interface. Sarkar [2003] related the anisotropic parameters and magnitude of the principal stress by non-linear elasticity theory. Recently, Pang [2020] derived the frequency-dependent PP and PS reflection coefficients with the changes of different incidence angles in the fractured medium. Xu et al. [2021] and Chen et al. [2022b] used acoustoelasticity theory and linear-slip theory to simulate reflection and transmission change with different incident angles under vertical static stress in a perfectly elastic formation under the condition of a non-welded interface. Furthermore, for these complex media, the corresponding reflection and transmission equations are further proposed [Worthington, 2010; Cui, 2017; Manogharan, 2021; Liu, 2012; Chen et al., 2022b]. However, the accurate reflection and transmission equations for the non-welded interface of the elasto-plastic medium under vertical stress are seldom studied. To better predict the properties of subsurface media and calculate the influence of the elasto-plastic on wave propagation. It is necessary to construct an accurate equation based on the elasto-plastic deformation medium, considering the non-welded interface and vertical stress conditions.

To fill this gap, we proposed accurate reflection and transmission equations suitable for stress-loaded elasto-plastic strata incident by plane P-wave on the non-welded interface. We use acoustoelasticity theory to describe the wave propagation under vertical overburden stress and the hardening parameter and plastic strain to describe elasto-plastic deformation. Meanwhile, we apply the linear-slip theory to model non-welded interfaces, where the stress is continuous but the displacement is discontinuous, and the difference in displacement across the interface is proportional to the stress [Schoenberg, 1980, 1988; Chaisri, 2000; Janaki Vamaraju, 2020; Chen, 2022b]. In this paper, we made the following assumptions: (1) The strata are thin, the P-wave wavelength is much larger than the interface thickness; (2) the disturbance of the plane P-wave is minimal and does not produce plastic deformation; (3) the deformation in all directions is small and can be approximated as a linear relationship, which is a linear simplification of the equation. This article investigated the influence of the elasto-plastic deformation medium on the amplitude and energy attenuation of reflected and transmitted waves under different incident angles and frequencies. Besides, we analyzed the dependence of wave reflection and transmission on fracture compliance hardening parameters, wave frequency, and incident angle in detail. The proposed equations can well explain the energy attenuation, high-frequency information loss, and abnormal reflections of reflected waves underground.

2. AOUSTOELASTICITY FOR ELASTO-PLASTIC DEFORMATION MEDIUM

Acoustoelasticity theory is a theory based on the theory of continuum and nonlinear wave theory [Pao et al., 1984; Man, 1987; Schoenberg, 1988; Traylor, 2021]. Which generally describes the wave velocity difference between the

observed object as static stress loaded and no force applied [Castellano, 2016]. In the case of studying large static deformations and superimposing small disturbances, the speed of the wave will change when there is stress acting on the propagating medium [Toupin et al., 1961; Turston et al., 1964; Chen, 2021b; Traylor, 2021]. This phenomenon can represent the wave propagation characteristics under the action of static stress [Pao et al., 1984; Man, 1987; Sarkar, 2003; Chen, 2021c, 2022a]. An isotropy rock loaded with stress will turn into anisotropy. This anisotropy is called stress-induced anisotropy, and in this paper, it is assumed that the medium in the two half-spaces is homogeneous and isotropic before static stress [Sarkar, 2003; Johnson, 1996]. Based on this theory, this chapter mainly introduces the acoustoelasticity theory of elasto-plastic deformation medium.

In the frame of acoustoelasticity theory, solids can be divided into three states, the unstressed natural state, the initial state after applying static stress, and the final state after receiving wave perturbation, as shown in Figure 1.

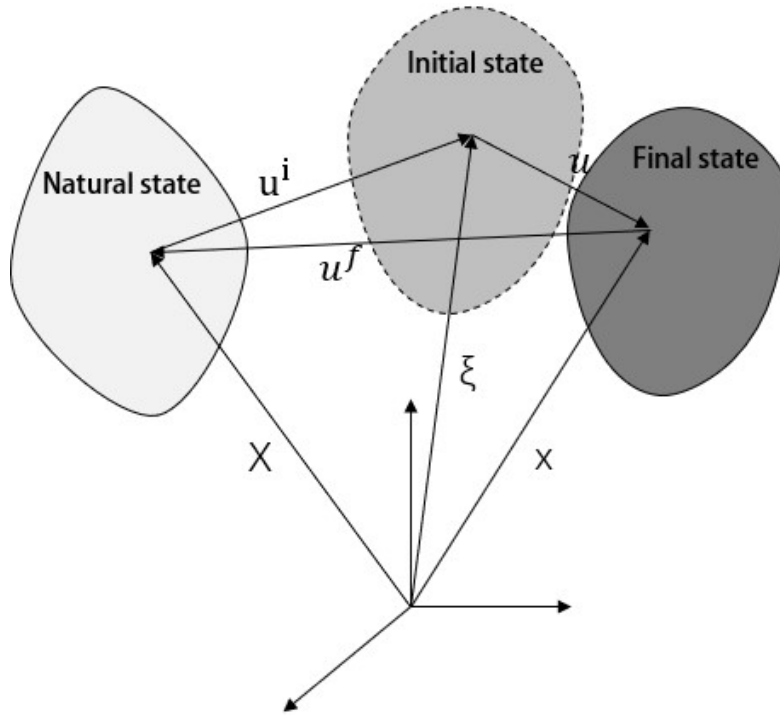


Figure 1. Three states of object particle under acoustoelasticity theory.

The natural state, initial state, and final state are denoted by X , ξ , and x , respectively. In the natural state, the parameter components in the natural state are represented by Roman capital letters. The Greek letter subscript represents this paper's initial state to represent the initial state's parameter component. A lowercase Roman letter subscript represents the final state, indicating the current configuration involved quantity components.

When it is assumed that the formation medium is an elasto-plastic deformation medium, its basic calculation is consistent with the calculation of the acoustoelasticity theory of elastic medium. According to the elasto-plastic deformation medium theory [Green and Naghdi, 1966a, 1966b], a new primary variable E^p is introduced, which is called the plastic strain. Its characteristics are: (1) It is a symmetric tensor; (2) It has the same invariance as the principal strain; (3) When the stress is over, the plastic strain is equal to the total strain, and the rate of change of the plastic strain does not depend on time. The main theory of elasto-plastic deformation medium theory is based on isothermal conditions. In elasto-plastic deformation theory, the existence of a hardening parameter γ is assumed, which represents a measure of the increase in hardness and strength due to plastic deformation and defined by the yield strength function f

$$\gamma = f(S_{AB}, E_{AB}^p). \quad (1)$$

Increase of hardening parameter means increase of plastic strain. And the elasto-plastic hypothesis satisfies

$$E_{AB}^e = E_{AB}^t - E_{AB}^p. \quad (2)$$

Elastic strain is the difference between total strain and plastic strain. The superscripts e , t , and p represent the static elastic strain, total strain, and plastic strain, respectively.

When considering wave propagation in a plastic medium, it is generally considered that a wave is an infinitely small disturbance that does not cause plastic deformation. Therefore, only the initial static stress can cause plastic deformation. According to the theory of segment calculation, the stress can also be divided into the initial stress and the later disturbance, and the second order of Piola-Kirchhof stress in the initial state can be obtained. After the linearization of u , S is expressed as [Liu, 2007; Sinha, 2001]:

$$S_{AB}^c = S_{AB} + \rho_0 F_{\alpha C} F_{\beta D} \frac{\partial^2 \psi}{\partial E_{AB} \partial E_{CD}} u_{\alpha, \beta}. \quad (3)$$

Where S represents the second order of Piola-Kirchhof stress, ψ is the free energy, and ρ_0 represents the density of matter in the natural state. The superscript c represents the final state. Because there is a conversion relationship between the Cauchy stress and the second order of Piola-Kirchhof stress in the final state, the Cauchy stress in the final state can be expressed as [Green and Naghdi, 1966a, 1966b; Pao et al., 1984; Ren 2022]:

$$\tau_{ij}^c = (\rho^c / \rho_0) F_{iA}^c F_{jB}^c S_{AB}^c, \quad (4)$$

where F is the deformation gradient. After simplify, which can be written as

$$\tau_{ij}^c = \tau_{ij}(1 - u_{m,m}) + \tau_{il} u_{j,l} + \tau_{kl} u_{i,k} + C_{ijkl} u_{k,l}, \quad (5)$$

where C can be expressed as:

$$C_{ijkl} = \rho F_{iA} F_{jB} F_{kC} F_{lD} \frac{\partial^2 \psi}{\partial E_{AB} \partial E_{CD}}. \quad (6)$$

This paper uses the free energy expression to determine the initial stress and elastic modulus C under elasto-plastic conditions [Sinha, 2001] and assumes that the plastic deformation does not affect the free energy. Its form can be written as:

$$\rho_0 \psi = c^{(0)} + c_{AB}^{(1)} E_{AB}^e + \frac{1}{2} c_{ABCD}^{(2)} E_{AB}^e E_{CD}^e + \frac{1}{6} c_{ABCDEF}^{(3)} E_{AB}^e E_{CD}^e E_{EF}^e. \quad (7)$$

Among them, c is the elastic constant. According to the hypothetical, when there is no elastic strain, the free energy should be zero, so $c^{(0)}$ is zero. Due to the third property of E^p , it can be inferred that $c^{(1)}$ is also zero. The remaining c becomes the second and third-order elastic moduli.

After simplification, the expression of elastic modulus and static stress can be obtained:

$$C_{ijkl} = (\rho/\rho_0)F_{iA}F_{jB}F_{kC}F_{lD}(c_{ABCD} + c_{ABCDEF}E_{EF}^e), \quad (8)$$

$$\tau_{il} = (\rho/\rho_0)F_{iA}F_{lB} \left(c_{ABCD}E_{CD}^e + \frac{1}{2}c_{ABCDEF}E_{CD}^eE_{EF}^e \right). \quad (9)$$

With the action of stress, the density of the formation will also change, and its change equation is shown in Eq. (10):

$$\rho \approx \rho_0(1 - e_{MM}^i). \quad (10)$$

At the same time, the speed will also change with the stress, and its change form is shown in Eq. (11-12):

$$V_P = \sqrt{\frac{\lambda + 2\mu + c_{112}(e_{11}^i + e_{22}^i) + (c_{111} - c_{123})e_{33}^i}{\rho}}, \quad (11)$$

$$V_S = \sqrt{\frac{\mu + (c_{112} - c_{123})e_{11}^i/2 + (c_{111} - c_{112})(e_{22}^i + e_{33}^i)/4}{\rho}}. \quad (12)$$

Eq. (11-12) are introduced into the equation by the action of plasticity through e^i . When the medium is fully elastic, the velocity expressions for longitudinal and transverse waves degenerate into: $V_{P0} = \sqrt{\frac{\lambda + 2\mu}{\rho}}$, $V_{S0} = \sqrt{\frac{\mu}{\rho}}$.

3. THE LINEAR-SLIP THEORY

The linear-slip method [Schoenberg, 1980; Worton, 2010] is used in this paper to describe non-welded interfaces. The non-welded interfaces generally refer to fractures, faults, Etc. [Hudson, 1981; Pyrak-Nolte, 1990; Michael, 1995; Chaisri, 2000; Vamaraju, 2020; Pang, 2020; Manogharan, 2021]. The linear-slip method assumes that the stress is continuous in the boundary conditions and the displacement is discontinuous, but the displacement difference and stress of the upper and lower interfaces are linearly related [Pyrak-Nolte, 1990]. It can be expressed as

$$\Delta u = ZT, \quad (13)$$

$$(T_{3i})^{up} = (T_{3i})^{low} \quad i = 1,3. \quad (14)$$

Where $\Delta u = u_2 - u_1$, the displacement difference between the lower layer and the upper layer, T is the stress vector on the non-welded interface, the superscripts up and low refer to the parameters of the upper and lower media, respectively, Z is the structural compliance parameter, which can be expressed as [Michael, 1995]

$$Z_{ij} = \Delta_T \delta_{ij} + (\Delta_N - \Delta_T)n_i n_j, \quad (15)$$

where $\Delta_T = 1/k_T$, $\Delta_N = 1/k_N$, where k_N is the normal stiffness parameter of fracture, and k_T is the tangential stiffness parameter of fracture. n_i and n_j represent the vertical and tangential vector components perpendicular to the fracture, respectively.

Assuming that the fracture satisfies normal up-down symmetry and rotational symmetry, Z can be simplified as a matrix composed of normal phase compliance Δ_N and tangential compliance Δ_T so that it can be expressed as [Schoenberg and Douma, 1988; Zhang and Gao, 2009; Chen, 2022b]:

$$Z = \begin{pmatrix} \Delta_T & 0 & 0 \\ 0 & \Delta_T & 0 \\ 0 & 0 & \Delta_N \end{pmatrix}. \quad (16)$$

Since reflection and transmission occurs only in the $Z - X$ plane, Z can degenerate to

$$Z = \begin{pmatrix} \Delta_T & 0 \\ 0 & \Delta_N \end{pmatrix}. \quad (17)$$

Eq. (17) describes the discontinuity of the discontinuous interface of the $Z - X$ plane, which paves the way for the derivation of the next section.

4. ACCURATE EQUATIONS FOR AN ELASTO-PLASTIC DEFORMED MEDIUM

This paper mainly deduces the seismic wave reflection and transmission coefficients equation at the non-welded interface between two elasto-plastic deformation medium half-spaces under vertical stress, ignoring the existence of fluid in the interface. The results calculated by the equation describe the influence of the seismic wave on the reflection and transmission coefficients of the seismic wave when it passes through the non-welded interface. Moreover, it is assumed that the upper and lower media are homogeneous isotropic media before being stressed.

Assuming plane P-wave incident, only reflected P-wave, reflected SV-wave, transmitted P-wave, and transmitted SV-wave are generated at the interface. Afterward, it is assumed that the reflection only occurs on the $X - Z$

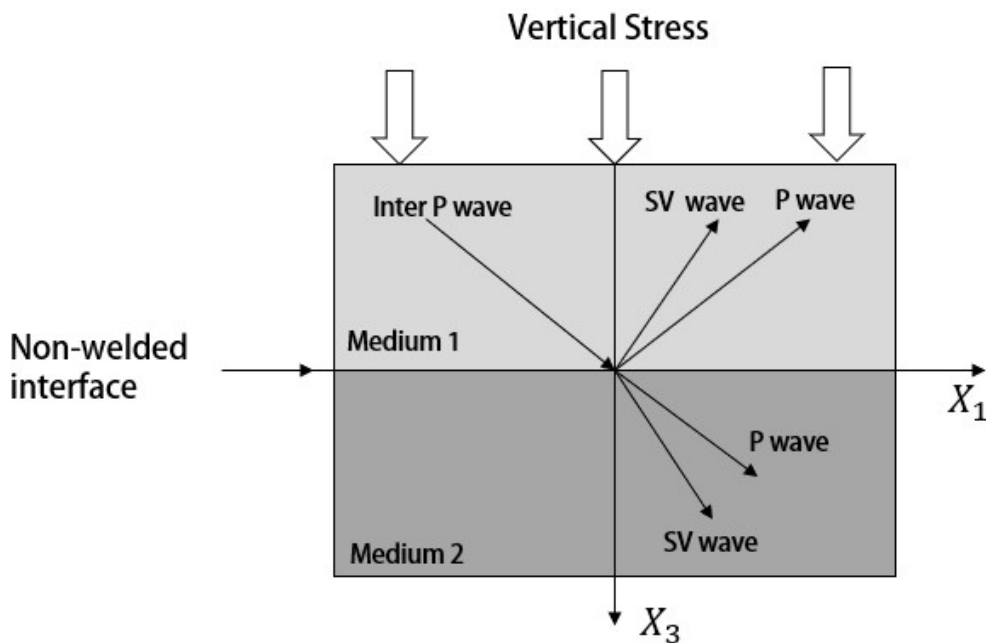


Figure 2. Schematic diagram of the transmitted and reflected waves generated by the plane P-wave incident interface.

plane [Liu, 2007; Chen 2021a, 2022a, 2022b]. As shown in Figure 2, the stress in other directions is zero. For the convenience of calculation, the displacement expression of the incident P-wave is expressed in terms of slowness, and the result is:

$$u_i^R = A^R P_i^R \exp[i\omega(m_j^R X_j) - t]. \quad (18)$$

Where A is the amplitude, P is the polarization vector, i is the imaginary part, t is the time, ω is the angular frequency, and satisfies the expression of $\omega = 2\pi f$, m is the slowness vector, and X is the pointing position information. Where R represents the type of wave, $R = 1, 2, 3, 4, 5$ represent reflected P-wave, reflected SV-wave, transmitted P-wave, and transmitted SV-wave. Subscripts I, J represent the vector direction of the wave, $I, J = 1, 3$.

According to the acoustoelasticity theory, the stress acting at the interface can be expressed by the first order of Piola-Kirchhof stress, which can be expressed as [Liu, 2007, Pao et al., 1984]:

$$T_{ij}^c = \tau_{ij} + C_{ijkl} e_{kl} + u_{i,k} \tau_{kj}, \quad (19)$$

T is the first type of Piola-Kirchhof stress, τ represents the initially applied static stress, if the medium is not subjected to the initial stress, this term is zero, e is the deformation due to wave propagation, which can be expressed as $e_{ij} = \frac{1}{2}(u_{i,j} + u_{j,i})$.

Combining acoustoelasticity theory, elasto-plastic deformation medium, and non-welded interfaces, the boundary conditions for those conditions can be written as:

$$\begin{cases} \left(\sum_{R=4}^5 u_1^R \right)_{X_3=0} = \left[\sum_{R=1}^3 (u_1^R + \Delta_T T_{31}^R) \right]_{X_3=0} \\ \left(\sum_{R=4}^5 u_3^R \right)_{X_3=0} = \left[\sum_{R=1}^3 (u_3^R + \Delta_T T_{33}^R) \right]_{X_3=0} \\ \left(\sum_{R=4}^5 T_{33}^R \right)_{X_3=0} = \left[\sum_{R=1}^3 (T_{33}^R) \right]_{X_3=0} \\ \left(\sum_{R=4}^5 T_{31}^R \right)_{X_3=0} = \left[\sum_{R=1}^3 (T_{31}^R) \right]_{X_3=0} \end{cases} \quad (20)$$

By solving the above equations, combining Eq. (18-20), the exact solution of the reflection and transmission coefficient at the non-welded interface of the elasto-plastic deformation medium can be obtained. Simplify the above equation to get:

$$LX = M; \quad (21)$$

$$L = \begin{pmatrix} L_{11} & L_{12} & L_{13} & L_{14} \\ L_{21} & L_{22} & L_{23} & L_{24} \\ L_{31} & L_{32} & L_{33} & L_{34} \\ L_{41} & L_{42} & L_{43} & L_{44} \end{pmatrix}; \quad (22)$$

$$X = [R_{PP}, R_{PS}, T_{PP}, T_{PS}]^T; \quad (23)$$

$$M = [M_{11}, M_{21}, M_{31}, M_{41}]^T. \quad (24)$$

Among them, L represents the stiffness matrix, and R_{PP} , R_{PS} , T_{PP} and T_{PS} represent the P-wave reflection coefficient, SV-wave reflection coefficient, P-wave transmission coefficient, and SV-wave transmission coefficient, respectively. The expression of each parameter in L is:

$$\begin{cases} L_{11} = P_1^2 + i\omega\Delta_T(C_{55}^{up}P_1^2m_3^2 + C_{55}^{up}P_3^2m_1^2) \\ L_{12} = P_1^3 + i\omega\Delta_T(C_{55}^{up}P_1^3m_3^3 + C_{55}^{up}P_3^3m_1^3) \\ L_{13} = P_1^4 \\ L_{14} = P_1^5 \end{cases}; \quad (25)$$

$$\begin{cases} L_{21} = P_3^2 + i\omega\Delta_N(C_{33}^{up}P_3^2m_3^2 + C_{31}^{up}P_1^2m_1^2 + P_3^2m_3^2\tau_{33}) \\ L_{22} = P_3^3 + i\omega\Delta_N(C_{33}^{up}P_3^3m_3^3 + C_{31}^{up}P_1^3m_1^3 + P_3^3m_3^3\tau_{33}) \\ L_{23} = P_3^4 \\ L_{24} = P_3^5 \end{cases}; \quad (26)$$

$$\begin{cases} L_{31} = i\omega(C_{33}^{up}P_3^2m_3^2 + C_{31}^{up}P_1^2m_1^2 + P_3^2m_3^2\tau_{33}) \\ L_{32} = i\omega(C_{33}^{up}P_3^3m_3^3 + C_{31}^{up}P_1^3m_1^3 + P_3^3m_3^3\tau_{33}) \\ L_{33} = -i\omega(C_{33}^{down}P_3^4m_3^4 + C_{31}^{down}P_1^4m_1^4 + P_3^4m_3^4\tau_{33}) \\ L_{34} = -i\omega(C_{33}^{down}P_3^5m_3^5 + C_{31}^{down}P_1^5m_1^5 + P_3^5m_3^5\tau_{33}) \end{cases}; \quad (27)$$

$$\begin{cases} L_{41} = i\omega C_{55}^{up}(P_3^2m_1^2 + P_1^2m_3^2) \\ L_{42} = i\omega C_{55}^{up}(P_3^3m_1^3 + P_1^3m_3^3) \\ L_{43} = i\omega C_{55}^{down}(P_3^4m_1^4 + P_1^4m_3^4) \\ L_{44} = i\omega C_{55}^{down}(P_3^5m_1^5 + P_1^5m_3^5) \end{cases}; \quad (28)$$

$$\begin{cases} M_{11} = -P_1^1 - i\omega\Delta_T C_{55}^{up}(P_3^1m_1^1 + P_1^1m_3^1) \\ M_{21} = -P_3^1 - i\omega\Delta_N(C_{33}^{up}P_3^1m_3^1 + C_{31}^{up}P_1^1m_1^1 + P_3^1m_3^1\tau_{33}) \\ M_{11} = -i\omega(C_{33}^{up}P_3^1m_3^1 + C_{31}^{up}P_1^1m_1^1 + P_3^1m_3^1\tau_{33}) \\ M_{11} = i\omega C_{55}^{up}(P_3^1m_1^1 + P_1^1m_3^1) \end{cases}. \quad (29)$$

It involves the polarity vector P and the slowness vector m , and the slowness vector and the polarization vector can be expressed as:

$$\begin{cases} P^1 = [\sin a_1, 0, \cos a_1], m^1 = [\sin a_1, 0, \cos a_1]/v_{P1} \\ P^2 = [\sin a_2, 0, -\cos a_2], m^2 = [\sin a_2, 0, -\cos a_2]/v_{P1} \\ P^3 = [\sin a_3, 0, \cos a_3], m^3 = [\sin a_3, 0, -\cos a_3]/v_{S1} \\ P^4 = [\sin a_4, 0, \cos a_4], m^4 = [\sin a_4, 0, \cos a_4]/v_{P2} \\ P^5 = [\cos a_5, 0, -\sin a_5], m^5 = [\sin a_5, 0, \cos a_5]/v_{S2} \end{cases}. \quad (30)$$

The function of the superscript is the same as R , which represents the type of wave. From 1 to 5, it represents the reflected P-wave, the reflected SV-wave, the transmitted P-wave, and the transmitted SV-wave, a_1 represents the angle between the incident P-wave and the Z axis, and a_2 represents the reflection. The angle between the P-wave and the Z axis, a_3 represents the angle between the reflected SV-wave and the Z axis, a_4 represents the angle between the transmitted P-wave and the Z axis, a_5 represents the angle between the transmitted SV-wave and the Z axis. Specifies that Z is vertical down in the positive direction. The calculation of P and m involves Snell's law and can be written as:

$$\frac{\sin a_1}{v_{P1}} = \frac{\sin a_2}{v_{P1}} = \frac{\sin a_3}{v_{S1}} = \frac{\sin a_4}{v_{P2}} = \frac{\sin a_5}{v_{P2}} = p, \quad (31)$$

p is the wave coefficient, which is an invariant constant. In the process of obtaining the L stiffness matrix, the calculation of C is involved, in which the subscripts use 11 1, 22→2, 33→3, 23→4, 13→5, 12→6. The final result obtained according to the elasto-plastic deformation theory, and acoustoelasticity theory is too complicated. Therefore, assumed that the elastic and plastic changes caused by waves are tiny and can be approximately regarded as linear and the elastic modulus can be seen at appendices.

Reflection and transmission discussed in this paper only occur in the $X - Z$ plane. When $E^t = 0$, there is no strain, and the equation can be regarded as the case where the elastic medium is not under stress. At this time, the equation can degenerate to the case where the vertical stress τ is zero [Chen 2022b]. When E^t is not zero, this equation can be regarded as the advancement of the elastic media equation in an elasto-plastic deformation medium because the elasto-plasticity of the medium is considered.

5. NUMERICAL RESULTS

In the process of solving the above equation, the formation parameters used in this study are shown in Table 1. E^t is used as a variable for analysis. Through the experimental study of Sinha [2001], we obtain E^p and E^e , and assumed that there is an approximate quadratic function relationship between E^p and E^t , which is displayed in Figure 3.

	ρ_0 (kg/m ³)	V_p (m/s)	V_s (m/s)	c_{144} (GPa)	c_{456} (GPa)	c_{123} (GPa)
A	2000	2000	1275	-162.5	-340.8	-95.9
B	2000	1437	984	-427.3	-240.9	-319.2

Table 1. Media parameters of Castlegate sandstone A and B.

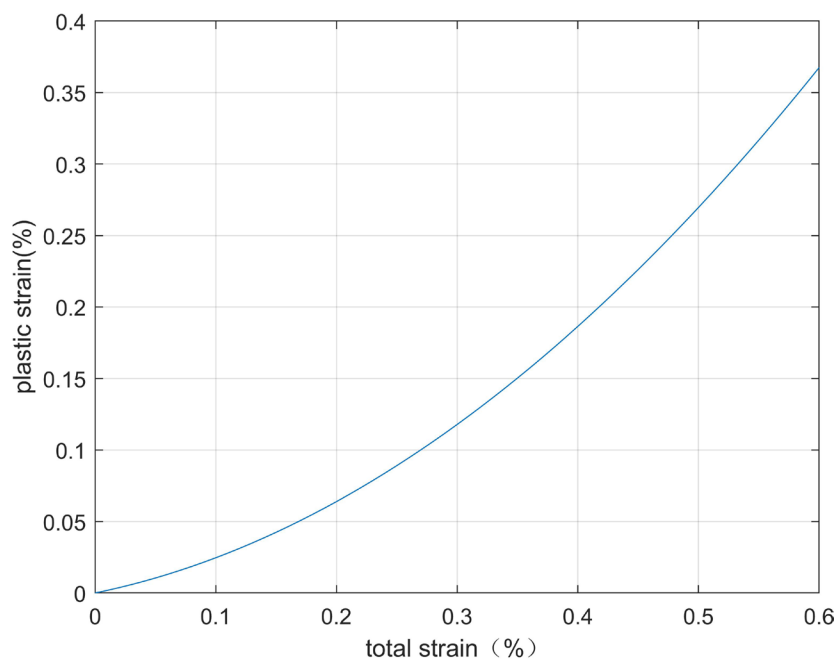


Figure 3. Relationship between total strain and plastic strain.

After E^p is obtained by $E^t - E^p$ relationship, all strains can be obtained by using $E^t = E^e + E^p$. After the total strain is changed, the strain can be substituted into the acoustoelastic equation to solve for the velocity of change due to stress. This paper assumes that the relationship between Δ_N and Δ_T can be written as $\Delta_T = 2\Delta_N$, and the normal compliance is given as $\Delta_N = 2.5 \times 10^{-9} (Mpa^{-1})$.

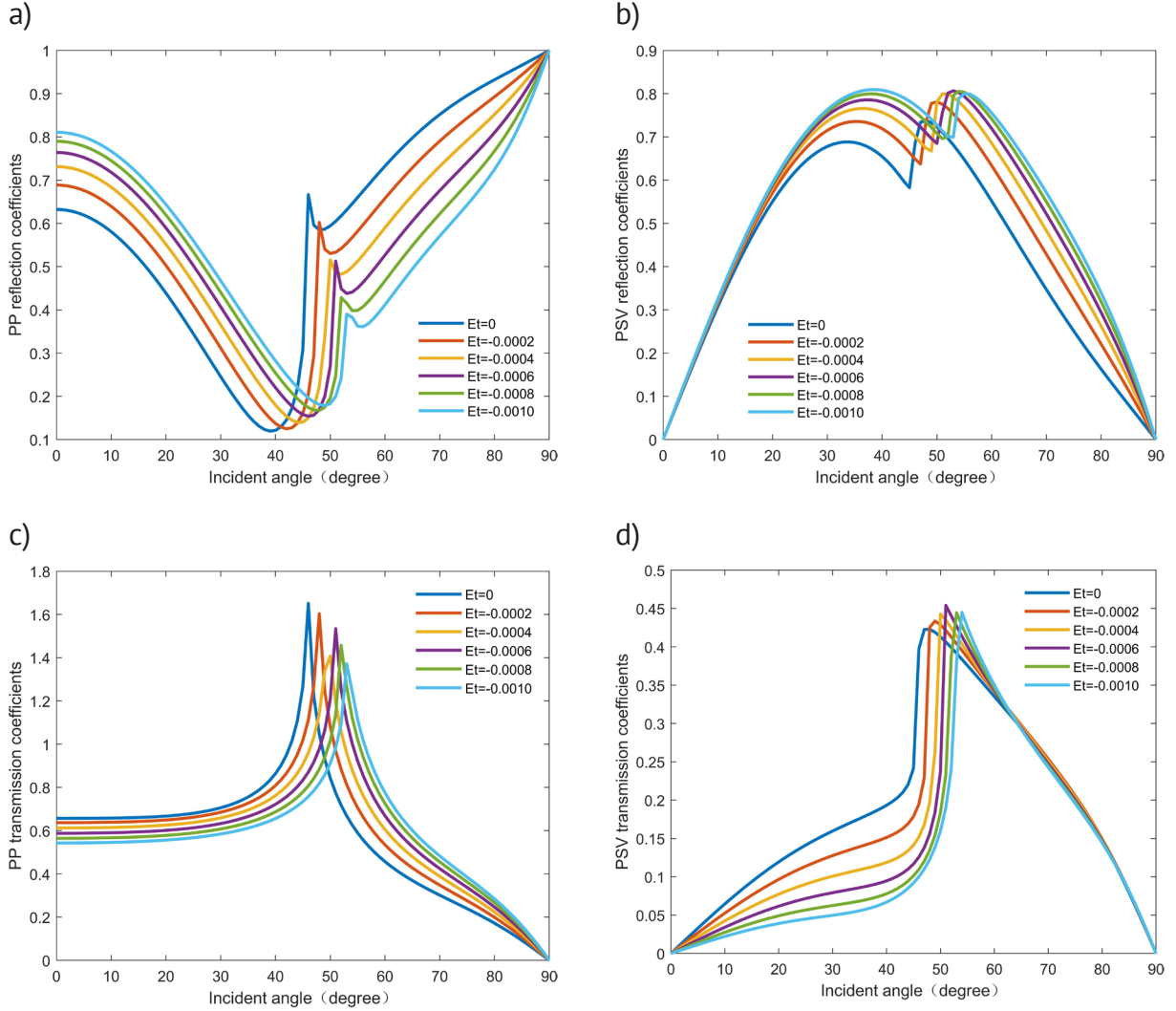


Figure 4. The relationship between incident angle and transmission coefficient and reflection coefficient, the frequency of incident P-wave is 30 Hz. (a) is the relationship between the incident angle and the reflection coefficient of the reflected P-wave; (b) is the relationship between the incidence angle and the reflection coefficient of the reflected SV-wave; (c) is the relationship between the incidence angle and the reflection coefficient of the transmitted P-wave; (d) is the relationship between the incident angle and the reflection coefficient of the transmitted SV-wave.

All the figures may have a curve mutation at the critical angle, and the critical angle moves right with the increase of E^t (the increase of E^t is the increase of absolute value, which is applied to full text). The general law of Figure 4 shows that except for R_{PP} , the other reflection and transmission coefficients show a trend of increasing first and then decreasing with the angle increase. At the critical and small or large angles, E^t appears to have little effect on some reflection or transmission coefficients. The reason may be that most of the energy is concentrated in the reflected P-wave, so E^t is basically no effect on the R_{PP} , R_{PS} , T_{PP} , T_{PS} at large angles. As we observe, with the increase of E^t , the peak amplitude of reflection goes low, and the transmission coefficient gets high.

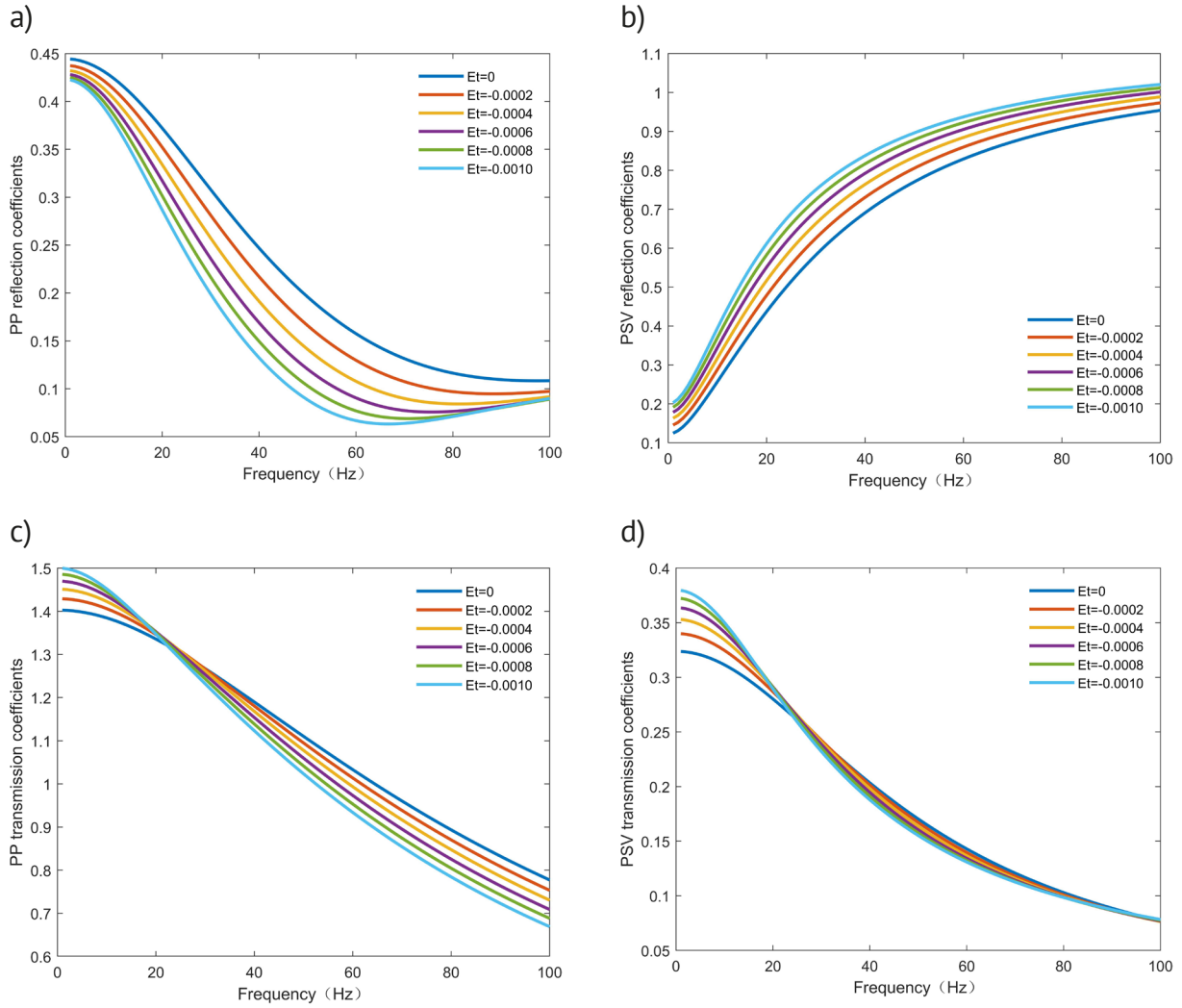


Figure 5. The relationship between the frequency of the incident P-wave and the transmission coefficient and reflection coefficient, the incident angle of the incident P-wave is 45° . (a-d) have a similar relationship with Figure 4.

In Figure 5, R_{PP} , T_{PP} and T_{PS} decrease with the frequency increase because the higher frequency has faster attenuation than low frequency, so R_{PP} , T_{PP} and T_{PS} will decrease at high frequency. In different E^t curves, the slope of the curve becomes large with the increase of E^t , indicating that the strain caused by the stress can increase the hardening parameter, weaken the effect of the non-welded interface increase the strata sensitivity of stress. The R_{PP} is more noticeable than the other coefficients because the upper layer is directly subjected to stress, not affected by non-welded interfaces. It is considered beneficial to generating reflected S-waves as the frequency increases. From different E^t curves of Figure 5, with the increase of E^t hardening parameter, R_{PS} show an increase, which means that with the increase of E^t and the hardening parameter, the formation becomes denser and will affect the S wave. From Figure 5d, with the increase of the hardening parameter, the slope of T_{PS} becomes large, which proves the attenuation effect of the compaction formation on the high-frequency decreases because the fracture in the strata is squeezed, which reduces the reduction of high-frequency energy.

From Figures 6, 7, 8 that all the changes of reflection and transmission coefficients are mainly concentrated when the normal compliance is between 10^{-10} and 10^{-5} . The change of the normal compliance increases, indicating that the normal stiffness of the fracture is smaller, and the stress required to generate unit displacement becomes smaller. In the figure, as the normal stiffness (normal compliance) of the fracture decreases, it means the division of the fracture becomes larger, which cause the effect of reflection increase, and the effect of transmission will decrease. When Δ_N is more than 10^{-5} , which can be approximately regarded as the interface between solid and air. Similarly, when Δ_N is less than 10^{-10} , the non-welded interface can degenerate into a welded interface.

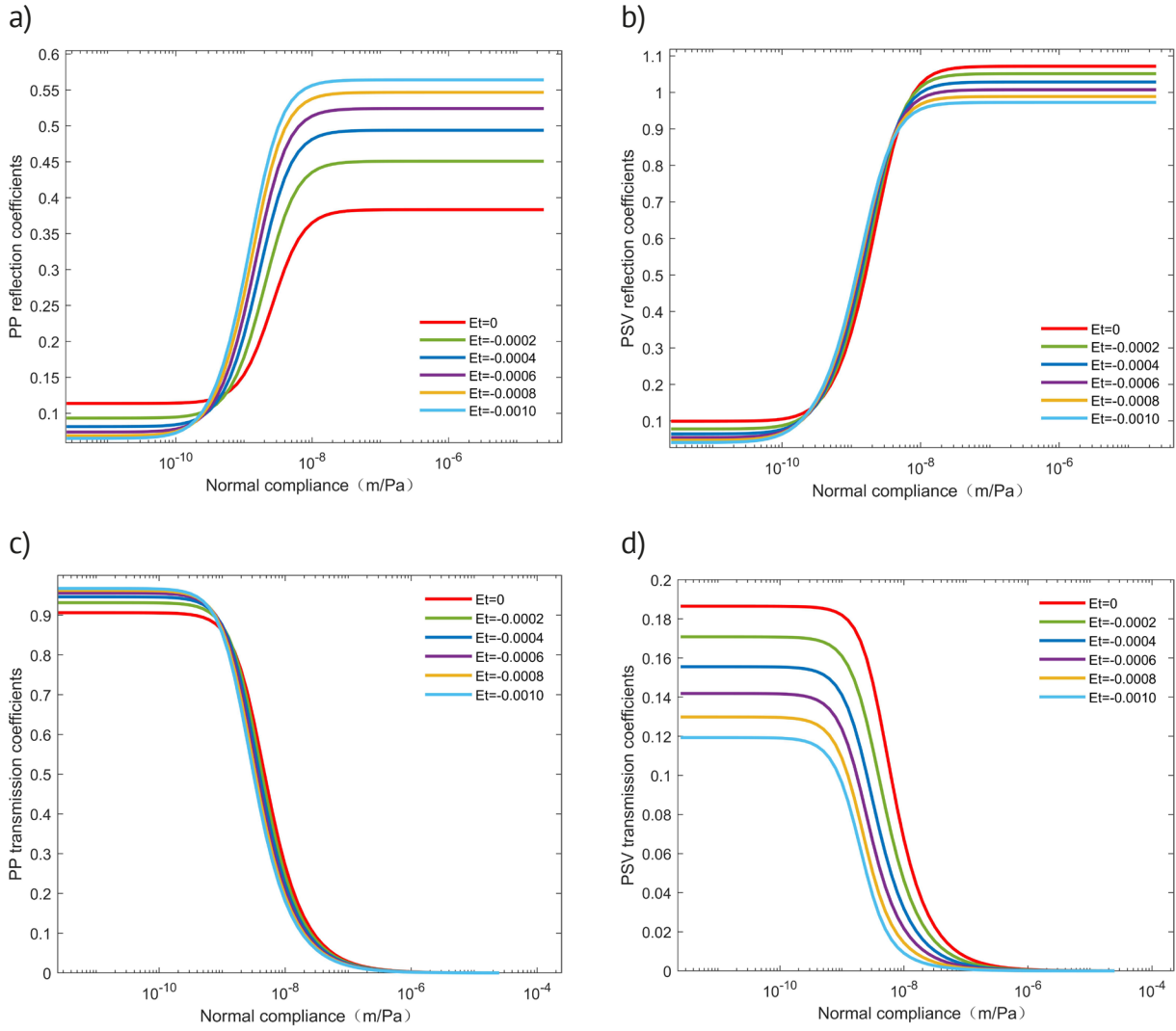


Figure 6. The relationship between the fracture normal compliance (Δ_N) and the transmission coefficient and reflection coefficient, the incident angle of the incident P-wave is 30° and the frequency is 60 Hz. (a) is the relationship between Δ_N and the reflection coefficient of reflected P-wave; (b) is the relationship between Δ_N and the reflection coefficient of reflected SV-wave; (c) is the relationship between Δ_N and the reflection coefficient of transmitted P-wave; (d) is the relationship between Δ_N and the reflection coefficient of the transmitted SV-wave.

From Figure 7, at the same E^t and Δ_N , the frequency will affect the whole curve shifted left and right, With the increase in frequency, the curves of R_{PP} , R_{PS} , T_{PP} , and T_{PS} will go left. From Figure 8, at the same E^t and Δ_N , the incident angle will make curves move up and down. In Figure 8a, above the critical angle, a large incident angle will make R_{PP} increase and slope decrease. From Figure 8b, the curves about 30° and 45° are almost the same, which proves that the S-wave splitting is stronger. At 60° , the influence of Δ_N is relatively small. In Figure 8c, the existence of the sliding wave at the critical angle causes the amplitude to be large. As the angle increases, T_{PP} becomes smaller for the other two angles. From Figure 8d, the overall amplitude increases with the increase of incident angle, and the curves go up. They indicated that small Δ_N is more beneficial for transmitted SV at large incident angles.

From Figures 6d,7d,8d, when the absolute value of E^t is greater than 0.0005, with the increase of E^t and hardening parameter, there is a certain promotion of fracture closure, so it will appear that T_{PS} becomes larger with the increase of E^t , which is conducive to the generation of S waves. However, the influence of Δ_N on T_{PS} is much more significant than E^t . The impact will eventually approach zero.

At Figures 9a, 9b, 9d, the reflection and transmission coefficient images are similar, indicating that the amplitude significantly influences the energy. The comparison of E^t in Figure 9c, with the increase of E^t , which makes the hardening parameter increase, the energy coefficients decrease but have almost no effect after the critical angle.

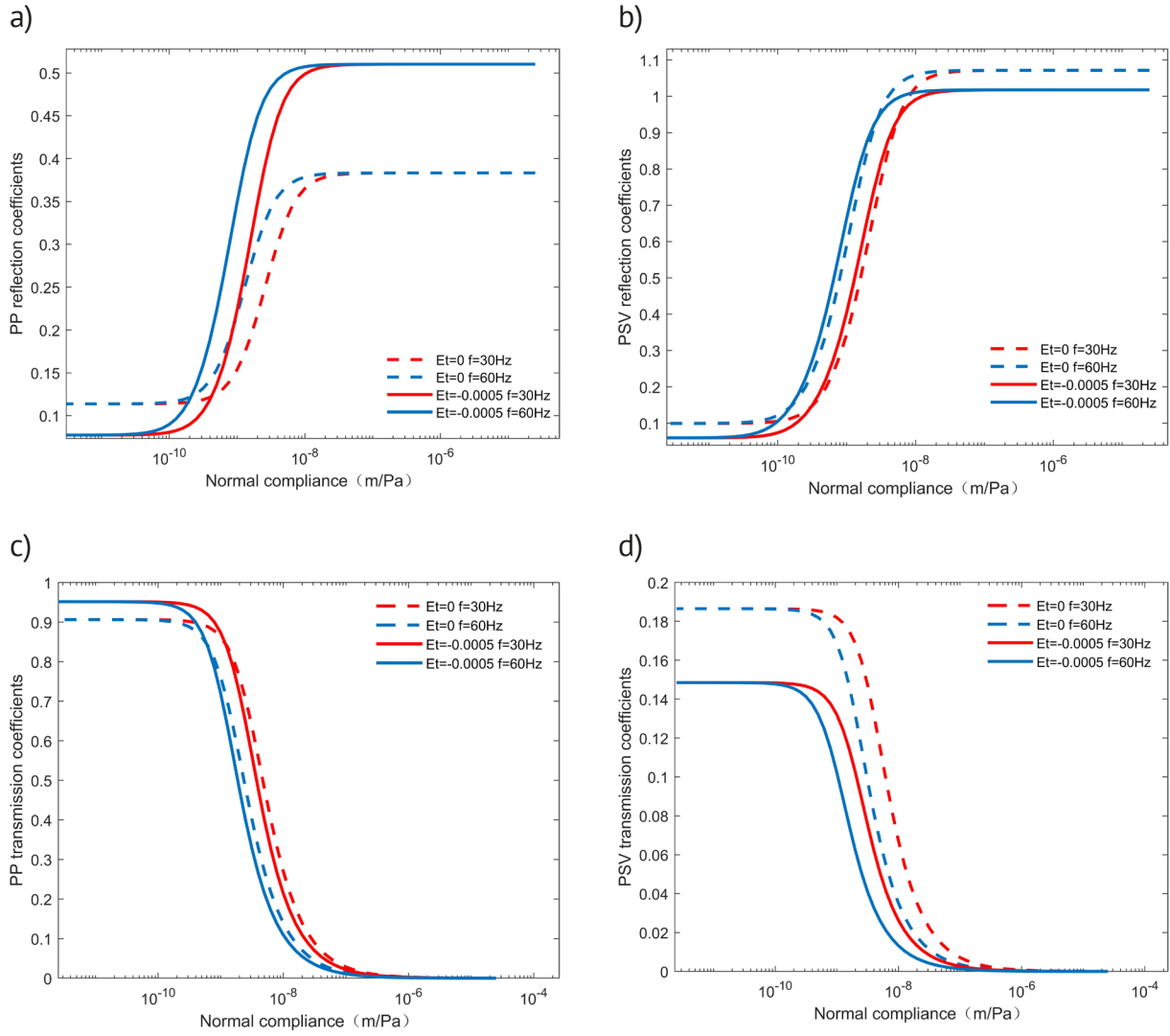


Figure 7. The relationship between the fracture compliance (Δ_N) and transmission coefficient and reflection coefficient. The incident angle of the incident P-wave is 30° , the frequency is 30 Hz and 60 Hz, and the total strain E^t is 0 and -0.0005 . (a-d) have a similar relationship with Figure 6.

Before the critical angle, the formation is dense due to the increasing hardening parameter, which is benefits to the transmission P-wave generation, so the transmission and reflectance energy coefficients are bigger. From Figure 9e, take curve $E^t = 0$ for example, before the critical angle, and after 60° , the reflected wave dominates the curves. The transmitted wave dominates curves from 45° to 60° . According to the comparison of different E^t , before the critical angle, E^t mainly affects reflected wave, and the law is opposite between 45° and 60° . After 60° , the strata tend to be dense, and the reflected wave energy dominates the curves. Figure 9e value is lower than 1. It is due to the energy consumption of non-welded surfaces and plasticity.

In Figure 10, $E^t = 0$ is non-welded by the degeneration of the equation in this paper; the unstressed non-welded interface is drawn according to the formula in Chaisri [2000]; the non-welded interface of the stressed elastic formation is drawn from Chen’s [2022b] data; the non-welded interface case of the stressed elasto-plastic formation is plotted by the formula in this paper. From the $E^t = 0$ curve in Figure 10, the formula derived in this paper is degenerate, and the result is consistent with the result of Chaisri [2000]. By observing the matching of the elasto-plastic and elastic cases deduced in this paper and the non-welded interface deduced by Chaisri [2000] without stress, it can be seen that the formula deduced in this paper also has applicability and correctness when $E^t > 0$. Moreover, as the absolute value of E^t decreases, the plastic deformation becomes smaller, and the three curves tend to overlap, which is also consistent with the actual cognition.

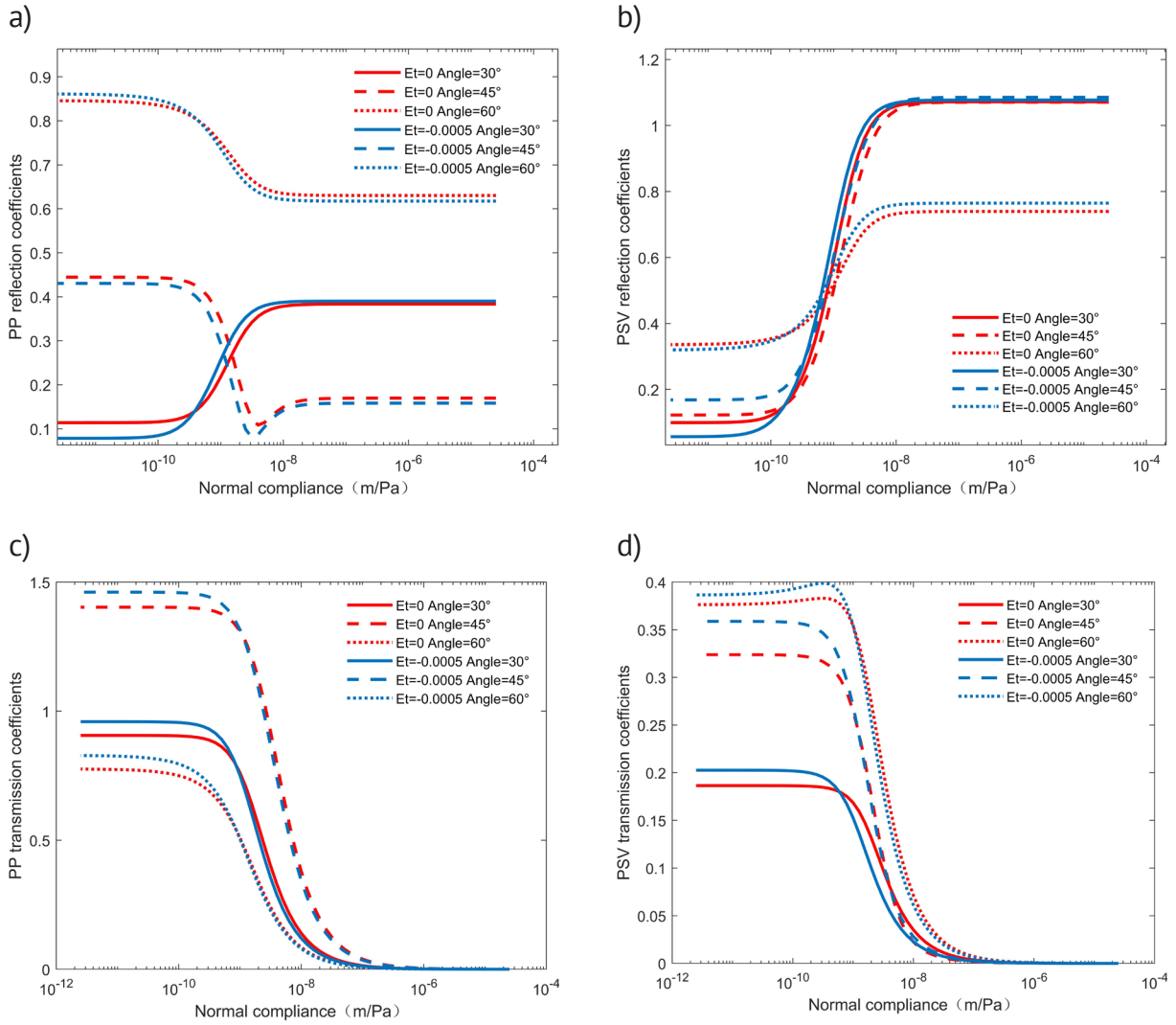


Figure 8. The relationship between the normal compliance (Δ_N) of the fracture and the transmission coefficient and reflection coefficient. The incident angle of the incident P-wave is 30°, 45°, 60°, the frequency is 60 Hz, and the total strain E^t is taken as 0 and -0.0005 . (a-d) have a similar relationship with Figure 6.

6. DISCUSSION

This equation can predict the accurate response of plane P-wave at the non-welded interface of elastic-plastic strata under stress. Compared with previous studies, this equation can achieve a more accurate prediction of wave response of underground interface. Through the analysis of the equation results, we can realize that the non-welded interface has a filtering effect on the incident wave. The stress can cause an increase in plasticity but also can weaken the impact of the non-welded interface.

At present, each of the three methods has a vital role in each area. The acoustoelasticity theory has been applied in logging wellbore pressure prediction and metal stress analysis. The elasto-plastic deformation and non-welded interface theories have already been widely used in reservoir prediction and fracture inversion in seismic exploration. However, due to high temperature and high pressure in deep strata, the rock tends to exhibit elasto-plastic characteristics in the actual product. After the rock cores leave the underground medium, the data measured in the laboratory experiment will cause significant deviation because it is no longer in the underground environment. Through the accurate equation derived in this paper, we can use the laboratory's pressure to infer the core's state when it is underground. After considering the elasto-plastic, it will be more reasonable and accurate to describe the subsurface non-welded transmission and reflection coefficients at the interface, achieving more precise reservoir inversion and fracture prediction.

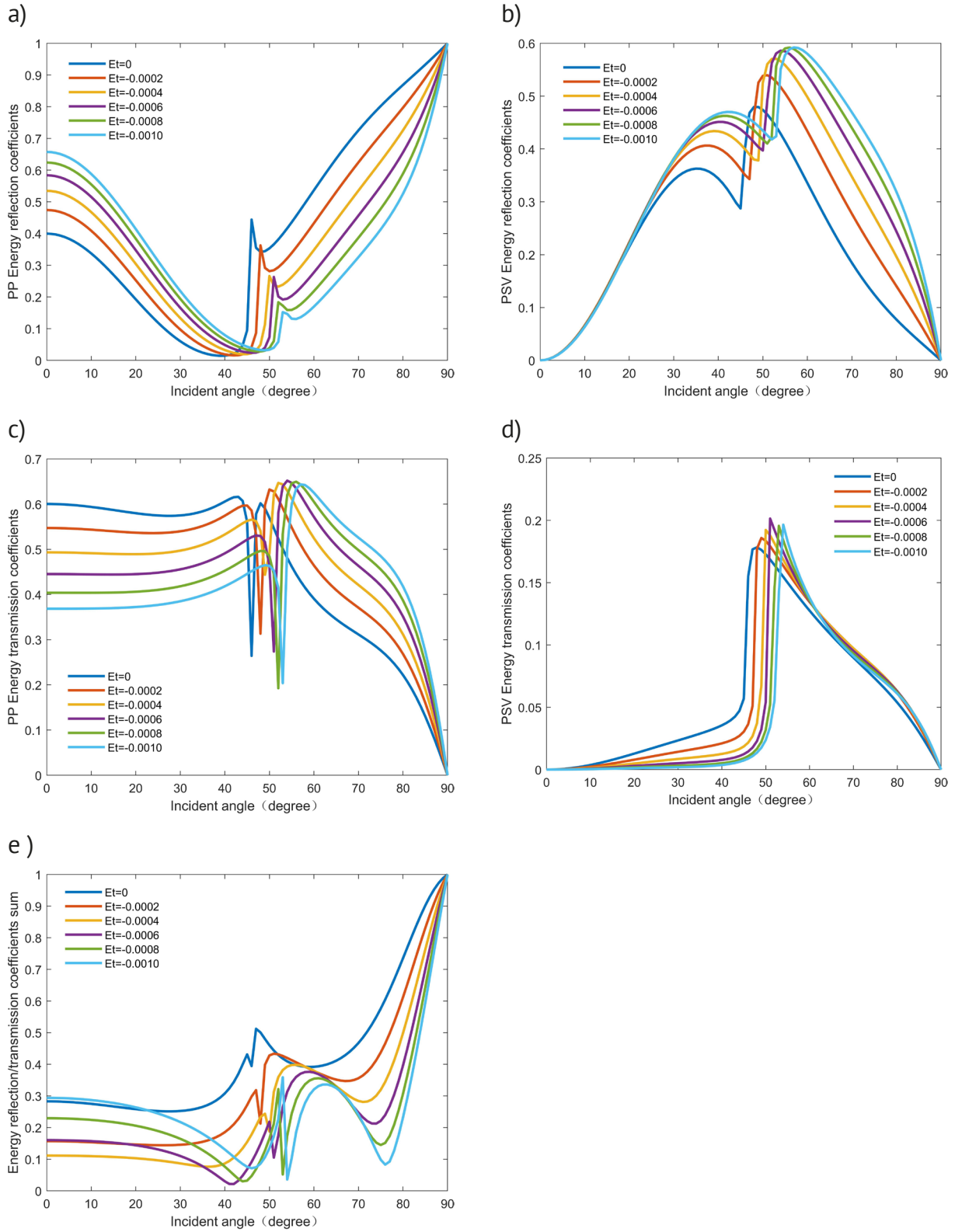


Figure 9. The relationship between incident angle and transmission and reflectance energy coefficients (the ratio of transmitted or reflected energy to incident energy), the incident angle of the incident P-wave is 30° , the frequency is 30 Hz, and the total strain E^t is taken from 0 to -0.001 . (a) is the relationship between the incident angle and the reflected P-wave ratio energy coefficient; (b) is the relationship between the incident angle and the reflected SV-wave ratio energy coefficient; (c) is the relationship between the incident angle and the transmitted P-wave ratio energy coefficient; (d) is the relationship between the incident angle and the energy coefficient of the transmitted SV wave ratio; (e) is the sum of the energy coefficients of the transmission and reflection coefficients under the same conditions.

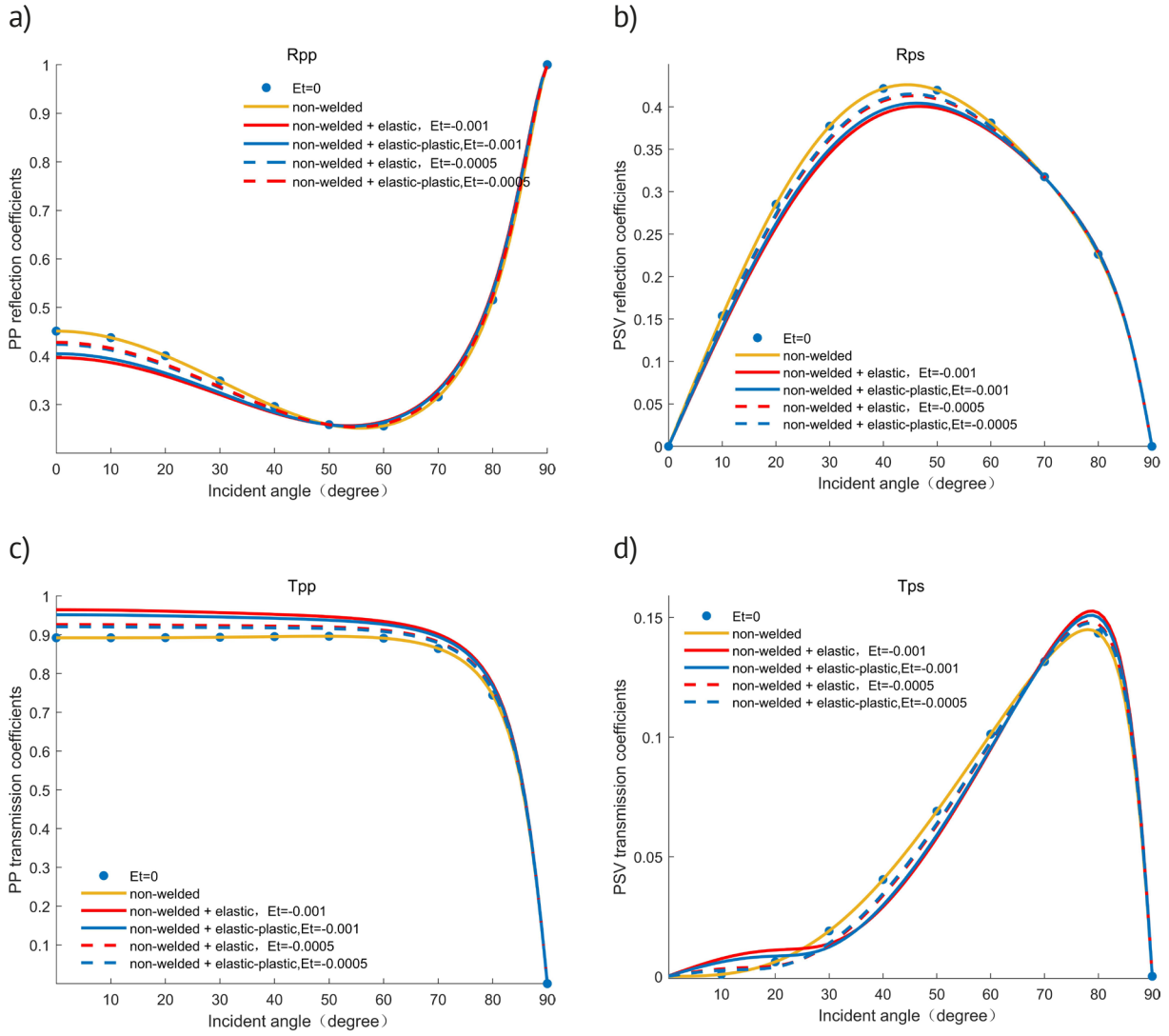


Figure 10. The relationship between incident angle and transmission and reflectance energy coefficients. Solid dot represents $E^t = 0$. Solid line represents non-welded case, non-welded interface of stressed elastic formation ($E^t = -0.001$), non-welded interface of stressed elasto-plastic formation ($E^t = -0.001$), respectively. Dotted line represents non-welded case, non-welded interface of stressed elastic formation ($E^t = -0.0005$), non-welded interface of stressed elasto-plastic formation ($E^t = -0.0005$), respectively. (a) is the amplitude of the reflected P-wave varies with the incident angle; (b) is the amplitude of the reflected SV wave varies with the incident angle; (c) is the amplitude of the transmitted P-wave varies with the incident angle; (d) is the amplitude of the transmitted SV wave as a function of the angle of incidence. The data are from Chaisri [2000].

However, there also have some problems that need to be solved. The equation in this paper is based on the quadratic approximation relationship between total strain and plastic strain. Linear approximation is used to simplify the calculation when calculating the stiffness matrix, so the linear approximation may not be applicable in more complex formations. The approximate relationship between the total strain and the plastic strain needs to be discussed in the strata with strong plasticity. In addition, when considering the non-welded interface in this paper, the specific filler in the fracture is not considered. When the fill in the fracture is highly viscous or has a strong absorbing effect on waves, the correctness of the equation results decreases. Meanwell, the acoustoelasticity theory has a problem in that the predicted elastic parameters, like velocity, will not converge at the high-stress regions, which implies that the prediction for reflection and transmission coefficient will not be promising in this case. Therefore, an uploaded acoustoelasticity model considering the high-stress limitation of wave velocity should be developed in the future research topic.

7. CONCLUSIONS

In this paper, the accurate equation of plane P-wave incidence at the uncoupled interface under stress is calculated, and the reflection and transmission of cracks under the background of the medium are obtained. Numerical results show that the change of E^t and hardening parameter caused by the stress leads to the change in the reflection and transmission coefficient. The effect of the non-welded interface on the R_{PP} , R_{PS} , T_{PP} , T_{PS} in terms of frequency is that the non-welded interface shows the low-pass filtering of the reflected P-wave and the transmitted wave, while the reflected SV wave shows the high-pass filtering. The increase of E^t will cause the hardening parameter to increase, frequency, and the slope of the R_{PP} , R_{PS} , T_{PP} , T_{PS} becomes larger. Meantime, an increase of E^t will increase the critical angle. The slope change can be inferred that the effects of the stress on the non-welded interface can be neutralized or reduced. As for the relationship between Δ_N and R_{PP} , R_{PS} , T_{PP} , T_{PS} related to the fracture properties, the non-welded interface is approximately close when $\Delta_N < 2.5 \times 10^{-10} (Mpa^{-1})$. When $\Delta_N = 2.5 \times 10^{-5} (Mpa^{-1})$, the fracture segmentation effect represented by the non-welded interface is noticeable, and the interface properties change from the solid-solid interface to approximately become a solid-air interface. Although E^t and hardening parameter has a weakening effect on the non-welded interface, the effect is not obvious. The frequency mainly leads curves to move left or right, while the angle makes curves move up or down. The non-welded interface has a strong attenuation effect on energy. Although the strain caused by the stress will weaken the attenuation effect of the non-welded interface, the influence of the non-welded interface on the formation is far more significant than the stress influence caused by strain. Finally, by using the data of Chen [2022b] and Chairri [2000], compared curves were drawn by this paper with other three situations, which are $E^t = 0$, non-welded interface, prestressed elastic non-welded interface, and prestressed elasto-plastic non-welded interface. Through those comparisons, we can prove that the equation derived by this paper is reasonably credible in both $E^t = 0$ and $E^t > 0$ situations.

8. APPENDICES

The elastic modulus of elasto-plastic acoustoelasticity are written as:

$$C_{11} = c_{11} + c_{11}(3E_{11}^t - E_{22}^t - E_{33}^t) + c_{111}E_{11}^e + c_{112}E_{22}^e + c_{112}E_{33}^e$$

$$C_{12} = c_{12} + c_{12}(E_{11}^t + E_{22}^t - E_{33}^t) + c_{112}E_{11}^e + c_{112}E_{22}^e + c_{123}E_{33}^e$$

$$C_{13} = c_{13} + c_{13}(E_{11}^t + E_{22}^t - E_{33}^t) + c_{112}E_{11}^e + c_{123}E_{22}^e + c_{112}E_{33}^e$$

$$C_{22} = c_{22} + c_{22}(3E_{22}^t - E_{11}^t - E_{33}^t) + c_{112}E_{11}^e + c_{111}E_{22}^e + c_{112}E_{33}^e$$

$$C_{23} = c_{23} + c_{23}(E_{22}^t + E_{33}^t - E_{11}^t) + c_{123}E_{11}^e + c_{112}E_{22}^e + c_{112}E_{33}^e$$

$$C_{33} = c_{33} + c_{33}(3E_{33}^t - E_{11}^t - E_{22}^t) + c_{112}E_{11}^e + c_{112}E_{22}^e + c_{111}E_{33}^e$$

$$C_{44} = c_{44} + c_{44}(E_{22}^t + E_{33}^t - E_{11}^t) + c_{144}E_{11}^e + c_{155}E_{22}^e + c_{155}E_{33}^e$$

$$C_{55} = c_{55} + c_{55}(E_{11}^t + E_{33}^t - E_{22}^t) + c_{155}E_{11}^e + c_{144}E_{22}^e + c_{155}E_{33}^e$$

$$C_{66} = c_{66} + c_{66}(E_{11}^t + E_{22}^t - E_{33}^t) + c_{155}E_{11}^e + c_{155}E_{22}^e + c_{144}E_{33}^e$$

$$\tau_{11} = c_{11}E_{11}^e + c_{12}E_{22}^e + c_{13}E_{33}^e$$

$$\tau_{22} = c_{12}E_{11}^e + c_{22}E_{22}^e + c_{23}E_{33}^e$$

$$\tau_{33} = c_{13}E_{11}^e + c_{23}E_{22}^e + c_{33}E_{33}^e$$

We ignoring the higher-order terms of the total strain and elastic strain. Only vertical stress τ_{33} exists in the stress τ . According to the analysis, just C_{33} , C_{13} , and C_{55} exist. The others are zero.

The relationship between the second and third-order elastic moduli can be sew at appendices [Pao et al. 1984; Hughes 1953]:

$$c_{155} = 2c_{456} + c_{144}; c_{112} = 2c_{144} + c_{123}; c_{111} = 4c_{155} + c_{112}$$

$$c_{11} = c_{22} = c_{33} = \lambda + 2\mu; c_{44} = c_{55} = c_{66} = \mu; c_{12} = c_{13} = c_{23} = \lambda$$

Acknowledgements. We sincerely thank the two anonymous reviewers for their constructive comments and suggestions on this paper, which will help me to conduct better research. We thank the sponsorship of National Natural Science Foundation of China (42030103,41974119, 42174139), Marine S&T Fund of Shandong Province for Pilot National Laboratory for Marine Science and Technology (Qingdao) (2021QNLMO20001-6) and Science Foundation from Innovation and Technology Support Program for Young Scientists in Colleges of Shandong province and Ministry of Science and Technology of China (2019RA2136).

Data availability statement. Data and code associated with this paper are available and can be obtained by contacting the corresponding author.

REFERENCES

- Backus G.E. (1962). Long-wave elastic anisotropy produced by horizontal layering, *J. Geophys. Res.*, 67, 4427-4440.
- Castellano A., P. Foti, A. Fraddosio et al. (2016). Monitoring applied and residual stress in materials and structures by non-destructive acoustoelastic techniques//2016 IEEE Workshop on Environmental, Energy, and Structural Monitoring Systems (EESMS). IEEE. 1-5.
- Chaisri S., E.S. Krebes (2000). Exact and approximate formulas for P-SV reflection and transmission coefficients for a nonwelded contact interface, *J. Geophys. Res.: Solid Earth*, 105, 28045-28054.
- Chen F., Z. Zong, M. Jiang (2021a). Seismic reflectivity and transmissivity parametrization with the effect of normal in situ stress, *Geophys. J. Int.*, 226, 1599-1614.
- Chen F., Z. Zong, X. Yin (2021b). Acoustoelastocity for joint effects of stress and thermal fields on wave dispersion and attenuation, *J. Geophys. Res.: Solid Earth*, 127, 2021JB023671.
- Chen F., Z. Zong (2021c). P-wave reflectivity parameterization for HTI medium with the effect of horizontal stress// First International Meeting for Applied Geoscience & Energy, Society of Exploration Geophysicists, 241-245.
- Chen F., Z. Zong, Y. Yang, X. Gu (2022a). AVO inversion using P-to S-wave velocity ratio and P-wave velocity, *Geophys.*, 87, 4, 1-74.
- Chen F., Z. Zong, X. Yin, et al. (2022b). Accurate formulae for P-wave reflectivity and transmissivity for a non-welded contact interface with the effect of in situ vertical stress, *Geophys. J. Int.*, 229, 311-327.
- Cui X, E.S. Krebes, L.R. Lines (2017). Seismic inversion for geologic fractures and fractured media. *Geophysics.*, 82, C145-C161.
- David E.C., R.W. Zimmerman (2012). Pore structure model for elastic wave velocities in fluid-saturated sandstones, *J. Geophys. Res.: Solid Earth.*, 117.
- Green A.E. and P.M. Naghdi (1966a). A general theory of an elasticplastic continuum, *Archives for Rational and Mechanical Analyses.*,18, 251-281.
- Green A.E. and P.M. Naghdi (1966b). A thermodynamic development of elasto-plastic continua//Irreversible aspects of continuum mechanics and transfer of physical characteristics in moving fluids. Springer, Vienna, 117-131.

- Hughes D.S., J.L. Kelly (1953). Second-Order Elastic Deformation of Solids, *Phys. Rev.*, 92, 1145.
- Hudson J.A. (1981). Wave speeds and attenuation of elastic waves in material containing cracks, *Geophys. J. Int.*, 64, 133-150.
- Johnson P.A., P. Rasolofosaon (1996). Nonlinear elasticity and stress-induced anisotropy in rock. *J. Geophys. Res.: Solid Earth.*, 101, 3113-3124.
- Liu J.X., Z.W. Cui, K.X. Wang (2007). Reflection and transmission of acoustic waves at the interface between rocks in the presence of elastic-plastic deformations, *J. Geophys. Engin.*, 4, 232.
- Liu J.X., Z.W. Cui, K.X. Wang (2012). Effect of stress on reflection and refraction of plane wave at the interface between fluid and stressed rock, *Soil Dyn. Earthqu. Engin.*, 42, 47-55.
- Man C.S., W.Y. Lu (1987). Towards an acoustoelastic theory for measurement of residual stress, *J. Elast.*, 17, 159-182.
- Manogharan P., C. Wood, C. Marone, D. Elsworth, J. Rivière, P. Shokouhi (2021). Nonlinear elastodynamic behavior of intact and fractured rock under in-situ stress and saturation conditions, *J. Mechan. Phys. Solids*, 153, 104491.
- Mulargia F. (1979). The evaluation of Murnaghan constants as a function of pressure, *Lett. Nuovo Cimento (1971-1985)*, 26, 471-476.
- Norris A.N. (1998). *Finite-Amplitude Waves in Solid Nonlinear Acoustics* ed M F Hamilton and D T Blackstock (New York: Academic), 263-76.
- Pang S., A. Stovas (2020). Frequency-dependent PP and PS reflection coefficients in fractured media, *Geophys. Prospect.*, 68, 926-940.
- Pyrak-Nolte L.J., L.R. Myer, N.G.W. Cook (1990). Transmission of seismic waves across single natural fractures, *J. Geophys. Res.: Solid Earth*, 95, 8617-8638.
- Ren C., J. Yu, S. Liu, W. Yao, Y. Zhu, X. Liu (2022). A Plastic Strain-Induced Damage Model of Porous Rock Suitable for Different Stress Paths, *Rock Mech. Rock Engin.*, 1-20.
- Sarkar D., A. Bakulin, R.L. Kranz (2003). Anisotropic inversion of seismic data for stressed media: Theory and a physical modeling study on Berea Sandstone, *Geophys.*, 68, 690-704.
- Schoenberg M. (1980). Elastic wave behavior across linear slip interfaces, *J. Acoust. Soc. Am.*, 68, 1516-1521.
- Schoenberg M., J. Douma (1988). Elastic wave propagation in media with parallel fractures and aligned fractures, *Geophys. Prosp.*, 36, 571-590
- Schoenberg M., C.M. Sayers (1995). Seismic anisotropy of fractured rock, *Geophys.*, 60, 204-211.
- Sinha B.K., T.J. Plona (2001). Wave propagation in rocks with elasto-plastic deformations, *Geophys.*, 66, 772-785.
- Traylor T.K., P.C. Burnley, M.L. Whitaker (2021). Initial Acoustoelastic Measurements in Olivine: Investigating the Effect of Stress on P- and S-Wave Velocities, *J. of Geophys. Res.: Solid Earth.*, 126, e2021JB022494.
- Vamaraju J., M.K. Sen, J. De Basabe, et al. (2020). A hybrid Galerkin finite element method for seismic wave propagation in fractured media, *Geophys. J. Int.*, 221, 857-878.
- Wang K., S. Peng, Y. Lu et al. (2021). Reflection coefficients of P-waves in partially saturated fractured media, *Geophys. Prosp.*, 69, 1678-1688.
- Worthington M.H, J.A. Hudson (2010). Fault properties from seismic Q, *Geophys. J. Royal Astron. Soc.*, 143, 937-944.
- Xu D., T. Han, L.Y. Fu (2021). Frequency-dependent seismic properties in layered and fractured rocks with partial saturation, *Geophys. Prosp.*, 69, 1716-1732.
- Yang H., L. Fu, B. Fu, et al. (2022). Acoustoelastic FD simulation of elastic wave propagation in prestressed media, *Front. Earth Sci.*, 501.

*CORRESPONDING AUTHOR: Zhaoyun ZONG,

School of Geosciences, China University of Petroleum (East China), Qingdao, China, 266580,
 Pilot National Laboratory for Marine Science and Technology (Qingdao), Qingdao, China,
 Shandong Provincial Key Laboratory of Deep Oil and Gas, Qingdao, China
 e-mail: zongzhaoyun@upc.edu.cn